THE ASTROPHYSICAL JOURNAL, 373:237–245, 1991 May 20

ANALYSIS OF RADIATION PRESSURE EFFECTS IN PULSATING STARS THROUGH PERTURBATIVE LIMIT CYCLE SOLUTIONS

A. COSTA & D. GÓMEZ[1]
Instituto de Astronomía y Física del Espacio (CONICET), Casilla de Correo 67, Sucursal 28, (1428) Buenos Aires, Argentina
AND
C. FERRO FONTÁN
Departamento de Física, Facultad de Ciencias Exactas y Naturales, Universidad de Buenos Aires, Ciudad Universitaria, (1428) Buenos Aires, Argentina
Received 1989 December 4; accepted 1990 November 2

ABSTRACT

We investigate the excitation and stability of limit cycle solutions of the one-zone model equations derived by Stellingwerf & Gautschy to demonstrate the usefulness of this approach and to gain understanding of radiation pressure effects on stellar pulsation. We use a perturbative analysis and discuss and compare the advantages of these techniques with the numerical integration of the equations. Interesting comparisons with observational data are found. The relationship of noise effects with irregularities of some types of stars is mentioned.

Subject headings: stars: interiors — stars: pulsation

1. INTRODUCTION

The excitation mechanism of oscillations in pulsating stars such as the Cepheids is a well-known phenomenon. However, some highly luminous pulsating stars, like the β Cephei variables, lie in a region of the Hertzsprung-Russell diagram which is shifted with respect to the theoretical predictions. It has been speculated that this shift is due to radiation pressure effects (Cox & Stellingwerf 1979).

In the present work we use a general set of equations describing a useful, but greatly simplified, one-zone pulsation model and explore the effects of radiation pressure on stellar pulsation. These equations have been derived by Stellingwerf & Gautschy (1988, hereafter SG88), who analyzed the effects of radiation pressure. We have developed a nonlinear perturbative calculation based on this set of three ordinary differential equations (ODEs) around its trivial (nonpulsating) equilibrium. Buchler & Goupil (1984) also developed a nonadiabatic perturbation formalism for stellar pulsation. Our study was motivated by the desire to study the effects of radiation pressure on pulsation.

The temporal behavior of a set of ODEs may be followed by looking at their trajectory in the space formed by the set of variables, usually known as phase space. In dissipative systems the long time evolution converges to a region of the phase space called attractor. In two-dimensional problems the system may be attracted to a fixed point (corresponding to a stationary equilibrium) or to a limit cycle (corresponding to a dynamic equilibrium or periodic solution). In three dimensions, besides these types of attractors we can also find tori or strange attractors. Generally this last kind of attractor is related to chaotic behavior of the system, that is, strong sensitivity to initial conditions. In conclusion, real systems exhibiting chaotic behavior are unpredictable in their long-term evolution, while if this is not the case the system converges to an attracting solution independently of the initial conditions. As a rule, the observed pulsation amplitudes of pulsating stars of a given type do not show great variations from star to star, indicating the existence of a nonlinear limit cycle type of behavior. However, some anomalous pulsating stars have been observed, suggesting the existence of strange attractors (Buchler & Kovacs 1987).

In this paper we identify regions of linear stability (instability) in a space formed by two free parameters. One of them (β) measures the relative importance of radiation and gas pressure, while the other one (ζ) is the ratio of luminous to thermal energy in the shell. The plane formed by these parameters resembles the H-R diagram. In this plane we also identify the regions where limit cycle attractors appear. Moreover, the behavior of these "dynamical equilibrium" states can roughly be typified by three quantities that depend on the two parameters mentioned above. They are the frequency, the amplitude, and the relaxation time toward the limit cycle. This information can be obtained by the numerical integration of the set of ODEs. However, the search for attractors necessarily involves long time integrations, and high accuracy is required, at least near the bifurcation point. On the other hand, a perturbative technique like the one we propose here presents the following advantages with respect to the numerical one:

1. The attractor, that is, the solution for times going to infinity, is directly obtained.
2. It gives a global view of the relevant characteristics of the limit cycles (stability, amplitude, shape, frequency, relaxation time, etc.) To obtain these features by the numerical method, one integration for each point in the parameters plane is required.
3. This method may be complemented by the direct numerical integration of the exact equations. However, it still gives useful orientation for the search for solutions of interest.

In § 2 we give a brief description of the model employed. In § 3.1 we introduce the mathematical basis of the perturbative method. In § 3.2 we apply this general technique to the present particular problem. In § 4 we show the results of some numerical integrations and compare them to the perturbative predictions. In § 5 we briefly enumerate our results and compare them with observations.

[1] Present address: Harvard Smithsonian Center for Astrophysics, 60 Garden Street, Cambridge, MA 02138.

2. THE MODEL

As we said above, we are interested in the analysis of the effects of radiation pressure in luminous pulsating stars. Before dealing with more sophisticated models, we decided in this paper to use the simplest model described in literature where this effect is considered (SG88) in order to study the main features of this phenomenon using our method. Moreover, as can be seen below, the simplicity of this model allows us to employ an analytical perturbative approach whose advantages will soon become evident.

The model derived by Stellingwerf & Gautschy (SG88) is a nonlinear generalization of the one-zone pulsation model of Baker (1966), where radiation effects are considered in the equation of state.

The set of dynamical equations is

$$dx/d\tau = y \,, \tag{2.1a}$$

$$dy/d\tau = (h+1)^{\chi_T}/(x+1)^q - 1/(x+1)^2 \,, \tag{2.1b}$$

$$dh/d\tau = [T_1\theta m(dx/d\tau) + T_2]/[\eta_T(x+1)^{(-m\theta)}(h+1)^{(\eta_T-1)}] \,, \tag{2.1c}$$

where x is the relative departure of the outer radius of the shell from the static equilibrium value, y is the velocity, h is a factor that contains the nonadiabatic effects as it is defined by Stellingwerf (1972). The time τ is measured in units of the free-fall time ($t_{\rm ff} = (R^3/GM)^{1/2}$, where R and M are the radius and mass of the star). The parameters involved in equations (2.1) define the structure of the pulsating shell as well as the thermodynamic characteristics of both gas and radiation. We adopted for them the standard values given by SG88 in their equations (1)–(22) and Table II excepting parameters β and ζ, which (as in SG88) are considered as free parameters in the present model.

The parameter β is

$$\beta = p_g/p \,, \tag{2.2}$$

where p_g is the gas pressure, p_r is the radiation pressure and $p = p_r + p_g$ denotes the total pressure.

The parameter ζ is

$$\zeta = L_0\, t_{\rm ff}/E_0\, M_s \,, \tag{2.3}$$

where L_0 is the equilibrium luminosity, E_0 is the internal energy per unit mass, and M_s is the total mass of the shell. Then ζ is the ratio of luminous to thermal energy of the shell.

3. PERTURBATIVE ANALYSIS

3.1. *General Method*

We shall describe now the perturbative technique applied to obtain the attractor of a set of equations near a bifurcation point. These points are intersections of attracting branches in phase space, and their importance relies on the fact that usually the stability of the attractors changes, thus transforming attractors into repellors. While this method is essentially based on Iooss & Joseph (1980), we have generalized it in order to obtain not only the equilibrium branches but also the nonlinear relaxation toward the stable ones (see also Gomez, Sicardi Schifino, & Ferro Fontán 1990).

Given a problem that can be described by a three-dimensional vector field $\boldsymbol{u}$ which evolves in time according to

$$\partial_i u_i = \mathscr{F}_i(\boldsymbol{u}, \beta, \zeta) \,, \tag{3.1}$$

where β and ζ are control parameters, the static equilibria are those $\boldsymbol{u}_0(\beta, \zeta)$ which solve

$$\mathscr{F}_i(\boldsymbol{u}_0(\beta, \zeta), \beta, \zeta) = 0 \,. \tag{3.2}$$

Performing a linearization of equation (3.1) around $\boldsymbol{u}_0(\beta, \zeta)$, the stability of these equilibria for each value of β and ζ can be found. Whenever the sign of the real part of one of the eigenvalues of the matrix $\partial_j \mathscr{F}_i(\boldsymbol{u}_0(\beta, \zeta), \beta, \zeta)$ becomes positive, the equilibrium $\boldsymbol{u}_0(\beta, \zeta)$ turns unstable. If a pair of eigenvalues are complex conjugate, a Hopf bifurcation arises for each $\beta_*(\zeta)$ where the real part of this pair of eigenvalues changes its sign. Hereafter we shall restrict ourselves to the study of this kind of bifurcations. As usual, we write down equation (3.1) in local form

$$\partial_i \psi_i = \mathscr{F}_i(\boldsymbol{\psi}, \mu, \zeta) \,, \tag{3.3a}$$

where the new vector field is

$$\boldsymbol{\psi} = \boldsymbol{u} - \boldsymbol{u}_0(\beta, \zeta) \,, \tag{3.3b}$$

and the control parameter is replaced by

$$\mu = \beta - \beta_*(\zeta) \,. \tag{3.3c}$$

Since we are interested in the search for new equilibria close to $\boldsymbol{u}_0(\beta, \zeta)$, we can work with the first terms of the Taylor expansion of the function $\mathscr{F}_i$ around $\psi_i = 0\,(i = 1, 2, 3)$. Thus

$$\partial_i \psi_i = \sum_{n=1}^{\infty} \frac{1}{n!}\, \partial^{(n)}_{j_1,\ldots,j_n} \mathscr{F}_i((\boldsymbol{u}_0(\beta_*, \zeta), \beta_*, \zeta)\psi_{j_1} \cdots \psi_{j_n} \,, \tag{3.4}$$

where the sum convention for the $j_k = 1, 2, 3$ has been used. As we shall see below, we must retain up to the third-order term to get a new equilibrium branch.

We are interested in considering the case where the eigenvalues of $L_{ij} = \partial_j \mathscr{F}_i$ are

$$\lambda_1 = \zeta + i\eta \,, \tag{3.5a}$$

$$\lambda_2 = \zeta - i\eta \,, \tag{3.5b}$$

$$\lambda_3 = \zeta' \,. \tag{3.5c}$$

We define the bifurcation curve $\beta = \beta_*(\zeta)$ as the set of points where ξ changes its sign.

The notation $|\phi_i\rangle$ indicates the eigenvector associated with λ_i and $\langle\phi_i|$ corresponds to the adjoint problem:

$$L|\phi_i\rangle = \lambda_i|\phi_i\rangle \,, \tag{3.6a}$$

$$\langle\phi_i|L = \lambda_i\langle\phi_i| \,. \tag{3.6b}$$

These eigenvectors satisfy the following orthonormal relations

$$\langle\phi_i|\phi_j\rangle = \delta_{ij} \,, \tag{3.7}$$

where the inner product is defined as $\langle A|B\rangle = \sum A_i B_i$.

Given that $\lambda_2 = \lambda_1^*$, then $|\phi_2\rangle = |\phi_1^*\rangle$ and $\langle\phi_2| = \langle\phi_1^*|$. Provided that $\lambda_3 = \lambda_3^*$, then $|\phi_3\rangle = |\phi_3^*\rangle$.

Any real vector $|\psi\rangle$ can be decomposed as

$$|\psi\rangle = \sum_{i=1}^{3} a_i|\phi_i\rangle \,, \tag{3.8}$$

and because of the properties written above, we find $a_2 = a_1^*$ and $a_3 = a_3^*$. In a completely general way, we can replace equation (3.8) into equation (3.4) and use the orthonormal relations (3.7) to obtain an evolution equation for the amplitudes $a_i(t)$. The third-order expressions in the Taylor expansion (3.4) are

$$\partial_t a_1 = (\xi + i\eta)a_1 + \sum_{\Sigma k_i = 2,3} (k_1, k_2, k_3)(a_1^{k_1})(a_2^{k_2})(a_3^{k_3}) \,, \tag{3.9a}$$

$$\partial_t a_3 = \xi' a_3 + \sum_{\Sigma k_i = 2,3} (k_1, k_2, k_3)'(a_1^{k_1})(a_2^{k_2})(a_3^{k_3}) \,, \tag{3.9b}$$

where the coefficients

$$(k_1, k_2, k_3) = \langle\phi_1|_i \frac{1}{n!}\partial^{(n)}_{j_1,\ldots,j_n}\mathscr{F}_i|\phi_1\rangle_{j_1}\cdots|\phi_1\rangle_{j_{k_1}}|\phi_2\rangle_{j_{k_1+1}}\cdots|\phi_2\rangle_{j_{k_1+k_2}}|\phi_3\rangle_{j_{k_1+k_2+1}}\cdots|\phi_3\rangle_{j_{k_1+k_2+k_3}} \,, \tag{3.10a}$$

$$(k_1, k_2, k_3)' = \langle\phi_3|_i \frac{1}{n!}\partial^{(n)}_{j_1,\ldots,j_n}\mathscr{F}_i|\phi_1\rangle_{j_1}\cdots|\phi_1\rangle_{j_{k_1}}|\phi_2\rangle_{j_{k_1+1}}\cdots|\phi_2\rangle_{j_{k_1+k_2}}|\phi_3\rangle_{j_{k_1+k_2+1}}\cdots|\phi_3\rangle_{j_{k_1+k_2+k_3}} \,, \tag{3.10b}$$

are the result of the contraction of the tensor $(1/n!)\partial^{(n)}_{j_1,\ldots,j_n}\mathscr{F}_i$ with k_i times the kets $|\phi_i\rangle$ $(i = 1, 2, 3)$ and once with the bras $\langle\phi_1|$ or $\langle\phi_3|$, depending of whether we consider (k_1, k_2, k_3) or $(k_1, k_2, k_3)'$. We shall now look for small-amplitude limit cycle solutions in the neighborhood of the bifurcation curve. Thus, we expand variables and control parameter in powers of a small parameter ϵ:

$$a_1(t) = A(t)\sum_{k=1}^{\infty} b_k(s)\epsilon^k \,, \qquad s = \omega(\epsilon)t \,, \tag{3.11a}$$

$$a_3(t) = \sum_{k=1}^{\infty} c_k(t)\epsilon^k \,, \tag{3.11b}$$

$$\omega(\epsilon) = \omega_0 + \sum_{k=1}^{\infty} \omega_{2k}\epsilon^{2k} \,, \tag{3.11c}$$

$$\partial_t A = \sum_{k=1}^{\infty} A'_{2k}\epsilon^{2k} \,, \tag{3.11d}$$

$$\mu(\epsilon) = \sum_{k=1}^{\infty} \mu_{2k}\epsilon^{2k} \,, \tag{3.11e}$$

and define ϵ as the amplitude of the limit cycle

$$\epsilon = \frac{1}{2\pi A}\int_0^{2\pi} ds\, e^{-is}a_1 = [a_1] \,. \tag{3.12}$$

Notice that $A(t)$ is a slowly varying function of t ($\partial_t A \propto \epsilon^2$), and thus the time integral in equation (3.12) can be performed assuming A equal to a constant. Moreover, A is defined so that $A \to 1$ for $t \to \infty$, recovering in that limit the expressions of Iooss & Joseph (1980). Note that for Hopf bifurcations ω, $\partial_t A$, and μ are even functions of ϵ (see eqs. [3.11c]–[3.11e]), as has rigorously been proved (Hassard, Kazarinoff, & Wan 1981).

Equations (3.9a)–(3.9b) transform into equalities between polynomials in ϵ, and thus they must hold at any order in ϵ. To first-order

$$\omega_0 \partial_s b_1 = i\eta b_1 , \tag{3.13a}$$

$$\partial_t c_1 = \xi' c_1 , \tag{3.13b}$$

hereafter parameters ξ, ξ', and η as well as all the coefficients (k_1, k_2, k_3) are evaluated at the bifurcation curve and then remain as functions of just one free parameter (ζ). We choose $\omega_0 = \eta$, and thus

$$b_1 = b_{10}\, e^{is} , \tag{3.14a}$$

$$c_1 = c_{10}\, e^{\xi' t} . \tag{3.14b}$$

According to equation (3.12) we have $[b_1] = b_{10} = 1$. To second-order

$$\omega_0 A(\partial_s b_2 - i b_2) = \sum_{\Sigma k_i = 2} (k_1, k_2, k_3)(Ab_1)^{k_1}(A^* b_1^*)^{k_2}(c_1)^{k_3} , \tag{3.15a}$$

$$\omega_0 A(\partial_s c_2 - i c_2) = \sum_{\Sigma k_i = 2} (k_1, k_2, k_3)'(Ab_1)^{k_1}(A^* b_1^*)^{k_2}(c_1)^{k_3} . \tag{3.15b}$$

At this point we are going to assume that $|\xi'| \gg \omega_0$, meaning that the relaxation toward the attractor manifold takes place in a typical time scale shorter than one period (see Fig. 1). Under this hypothesis we can approximate $e^{\xi' t} \approx 0$. The condition (3.12) is automatically satisfied by equation (3.15a). Notice that for any $k > 1$, condition (3.12) reads $[b_k] = 0$ and implies that equations of the type of equation (3.15a) can be solved whenever the right-hand side has no terms proportional to e^{is}. This solvability condition, also known as the Fredholm alternative, when applied to the different orders in ϵ, will provide equations from which ω_{2k}, A'_{2k} and μ_{2k} can be obtained. Following to third-order in ϵ, we find

$$\begin{aligned}\omega_0 A(\partial_s b_3 - i b_3) = & -\dot{A}_2 b_1 + \sum_{\Sigma k_i = 3} (k_1, k_2, k_3)(Ab_1)^{k_1}(A^* b_1^*)^{k_2}(c_1)^{k_3} \\ & + Ab_2((1, 1, 0)A^* b_1^* + (1, 0, 1)c_1) + A^* b_2^*((1, 1, 0)Ab_1 + (0, 1, 1)c_1) \\ & + c_2((1, 0, 1)Ab_1 + (0, 1, 1)A^* b_1^*) ,\end{aligned} \tag{3.16}$$

and an analog equation for $c_3(t)$. The solvability condition implies

$$\partial_t A \approx \dot{A}_2 \epsilon^2 = (\Gamma A - \Gamma' |A|^2 A)\epsilon^2 , \tag{3.17}$$

where

$$\Gamma = \xi_\mu \mu_2 + i(\eta_2 - \omega_2) , \tag{3.18a}$$

$$\begin{aligned}\Gamma' = & -2/3\,|(0, 2, 0)|^2/i\omega_0 + (2, 0, 0)(1, 1, 0)/i\omega_0 - (2, 1, 0) \\ & + (0, 1, 1)(2, 0, 0)'/\xi' + (1, 0, 1)(1, 1, 0)'/\xi' - |(1, 1, 0)|^2/i\omega_0 ,\end{aligned} \tag{3.18b}$$

and

$$\Gamma = \Gamma' , \tag{3.18c}$$

because of the condition $A \to 1$ for $t \to \infty$.

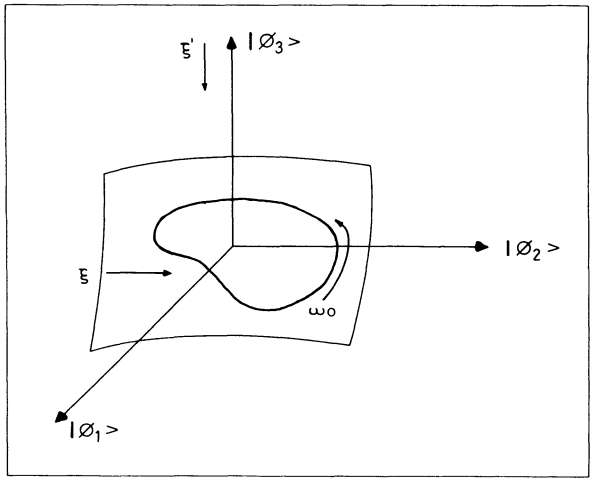

FIG. 1.—Characteristic frequencies associated with the two-dimensional manifold

It is straightforward to construct a function to analyze the stability of the limit cycle solution. Decomposing Γ' and A as

$$\Gamma' = \Gamma'_r + i\Gamma'_i , \tag{3.19a}$$

$$A = |A| e^{i\phi} , \tag{3.19b}$$

and taking the real part of equation (3.17), we get

$$\partial_t |A| = \Gamma'_r \epsilon^2 |A| (1 - |A|^2) . \tag{3.20}$$

We can write down this equation in the form

$$\partial_t |A| = -\partial S / \partial |A| , \tag{3.21}$$

where

$$S(|A|) = \frac{\Gamma' \epsilon^2}{2} |A|^2 \left(\frac{1 - |A|^2}{2} \right) \tag{3.22}$$

is a generalized potential in the sense that the equilibria of the system correspond to the extrema of this function, the minima being the stable ones (Haken 1983). This is so because equation (3.22) implies $\partial_t S \leq 0$ for all values of $|A|$.

3.2. *Application to the Model Equations*

For the case of equations (2.1a)–(2.1c), the components of the vector field ψ are

$$\psi_1 = x , \quad \psi_2 = y , \quad \psi_3 = h , \tag{3.23}$$

With two free parameters β and ζ defined above (eqs. [2.2]–[2.3]).

The linearized expression of equations (2.1a)–(2.1c) can be written as

$$\dot{\psi} = \boldsymbol{L}\psi , \tag{3.24}$$

with

$$\boldsymbol{L} = \begin{vmatrix} 0 & 1 & 0 \\ (2 - q) & 0 & \chi_T \\ \dfrac{-\xi(b - u)}{\eta} & 0 & \dfrac{-\xi(s + 4)}{\eta} \end{vmatrix} , \tag{3.25}$$

where χ_T, η, b, u, and s are the same as in (SG88).

The eigenvalues λ_1 and λ_2 are a pair of complex conjugate numbers associated with the pulsation, while λ_3 is real and negative and corresponds to the thermal cooling rate (see SG88). Thus, we are dealing with the spectral structure indicated in equation (3.5). In Figure 2 we show the region of linear stability (instability) of the trivial equilibrium corresponding to $\xi < 0$ ($\xi > 0$). The curve $\beta = \beta_*(\zeta)$ corresponding to $\xi = 0$ (neutral stability) is a quite smooth function of ζ and is approximately $\beta_* \approx 0.147$. The behavior of the pulsational frequency $\eta = \omega_0$ and the thermal cooling rate $|\xi'|$, both evaluated at the critical curve, is shown in Figure 3*a*. We want to notice that ω_0 is approximately independent of ζ and has the value $\omega_0 = 2.8$.

In order to search for limit cycle solutions in the linearly unstable region we include terms up to third order in ψ components. The tedious calculation of the brackets (k_1, k_2, k_3) as well as part of the perturbative expansion in ϵ that follows were performed with the aid of a symbolic manipulation program (SMP). Following the method described in the previous section from equation (3.8) onward, we obtain the first solvability condition (eq. [3.17]) at order ϵ^3. From the real and imaginary part of equation (3.18c) we can

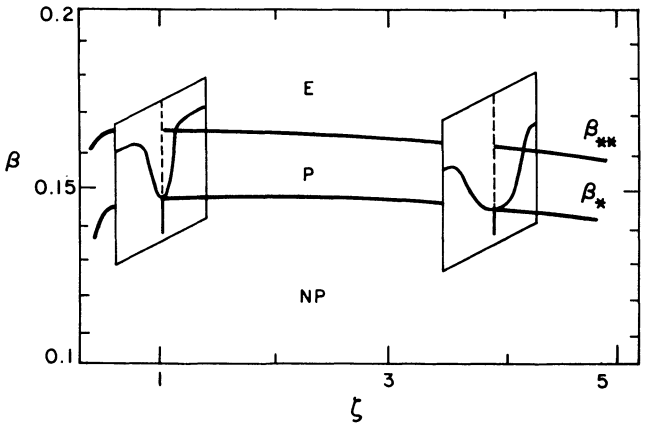

FIG. 2.—Critical curve β_* and curve for β_{**}, which divide the β-ζ plane into regions where stars either pulsate (P), do not pulsate (NP), or experience ejection (E) of the shell. The shape of the attractor in the β-x plane is also schematically shown.

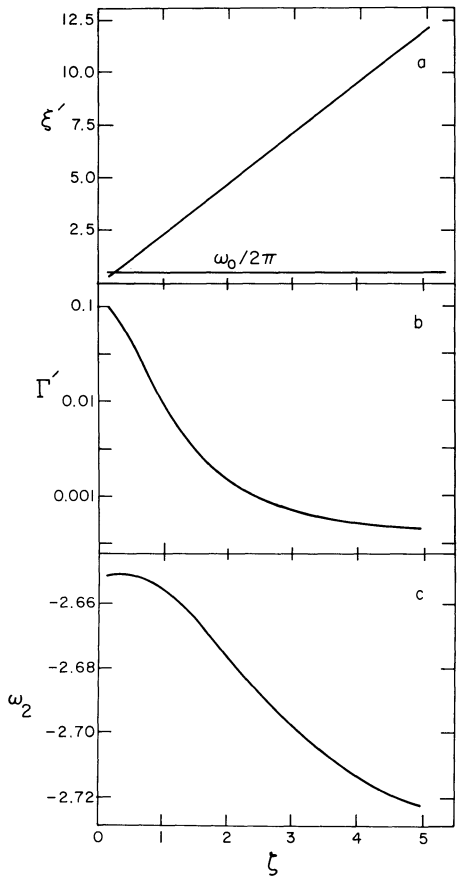

FIG. 3.—(*a*) Dependence of $|\xi'|$ (linear relaxation toward the manifold plane) and ω_0 on ζ. (*b*) Dependence of Γ' (relaxation toward the limit cycle attractor) on ζ. (*c*) Dependence of ω_2 with ζ.

derive μ_2 and ω_2 as functions of ζ:

$$\mu_2 = \Gamma_r'/\xi_\mu \,, \tag{3.26}$$

$$\omega_2 = \eta_2 - \Gamma_i' \,. \tag{3.27}$$

The sign of Γ_r' decides the stability of the limit cycle branch as well as its orientation. The function $\Gamma_r'(\zeta)$ is shown in Figure 3*b*. We obtain positive values for every ζ indicating that a stable supercritical Hopf bifurcation takes place, as it is schematically shown in Figure 2. In Figure 3*c* we show the dependence upon ζ of the nonlinear correction to the frequency (ω_2). Notice that for any ζ the correction ω_2 remains small and negative, implying that the pulsation frequency decreases as the value of β is raised ($\omega = \omega_0 + \omega_2 \epsilon^2$). In Figure 4 the dotted curves show the shape of the attractor for different values of β and ζ. In Figure 5*a*, we show the amplitude evolution $x_{\max}(t)$ ($x_{\max}$ is the maximum value of x in one period, corresponding to $\dot{y} = 0$ and $x > 0$) obtained from the analytical integration of equation (3.17). In both figures we compare these perturbative results with those derived from the numerical integration of the exact set of equations (see next section).

4. DIRECT NUMERICAL INTEGRATION

We numerically solve the exact set of equations (2.1a)–(2.1c) with a fourth-order Runge-Kutta method for different values of β and ζ and different values of initial conditions. The shape of the attractors and the relaxation time toward them compare qualitatively well with the perturbative results (see Figs. 4–5) (in Fig. 4 the perturbative case is the dotted curve and the numerical solution is the solid line). The fitting in Figure 4 improves as the value of β approaches the critical curve $\beta_* \approx 0.147$, as is expected for a perturbative calculation. As we said, in Figure 5 we show the evolution of the maximum of x with time in its relaxation toward the attractor (asymptotic value of x) for different values of β and different initial conditions (curves *a* and *b*; where *a* is initial condition from the outside of the attractor and *b* is initial condition from the inside of the attractor). We see that the relaxation time increases for values close to β_*. On the other hand, for β sufficiently higher than the critical one, we see in Figure 5*b*, that the relaxation time enlarges while the frequency diminishes (separation between dots in a curve is one period). For even higher values of β, the amplitude of variable y reaches the escape velocity, ($y \approx 1$) and there is no attracting solution. This evolution corresponds to the ejection of the pulsating shell (see Fig. 6*a*). Figures 6*b* and 6*c* show the ejection of the shell for different values of β. We notice that the rate of increase of the amplitude agrees with the linear result derived in SG88, where a maximum of the growth rate instability is found at $\beta = 0.7$.

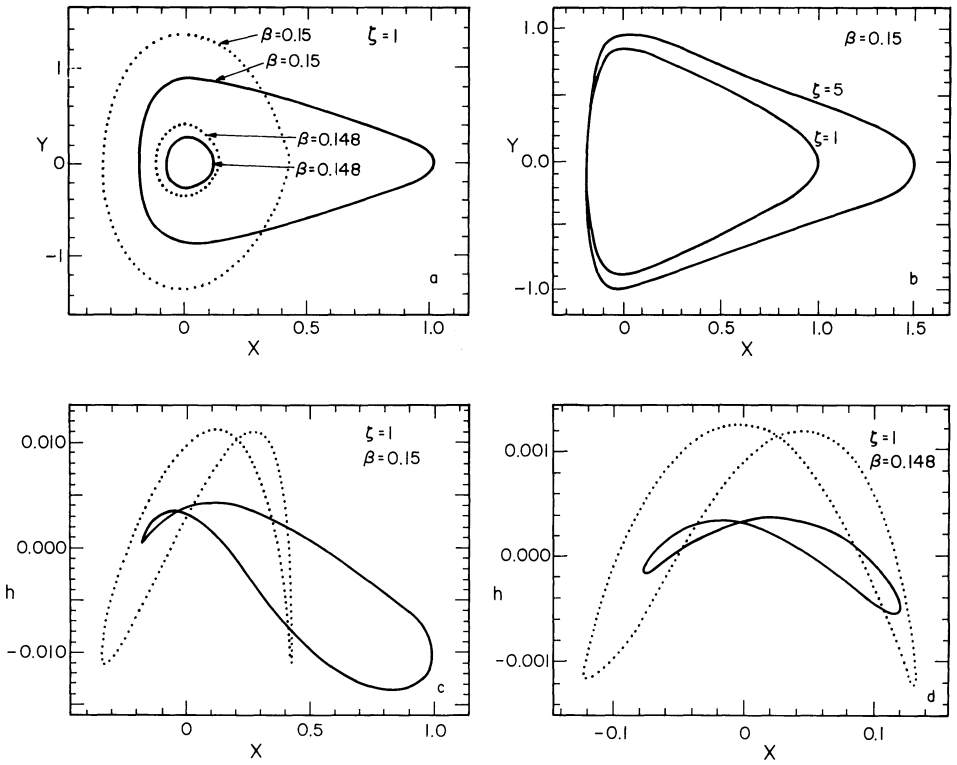

FIG. 4.—Dotted lines correspond to perturbative results and full lines correspond to numerical ones (*a*) Shape of the attractor in the *y*-*x* plane for $\zeta = 1$ with $\beta = 0.148$ and $\beta = 0.15$. (*b*) Shape of the attractor in the *h*-*x* plane for $\zeta = 1$ with $\beta = 0.148$. (*c*) Shape of the attractor in the *h*-*x* plane for $\zeta = 1$ with $\beta = 0.15$. (*d*) Shape of the attractor in the *y*-*x* plane for $\beta = 0.15$ with $\zeta = 1$ and $\zeta = 5$.

We also found that for values of $\beta > \beta_{**}$ (β_{**} depends weakly on m, for example $\beta_{**} \approx 0.18$ if $m = 10$), the ejection of the shell takes place at any value of ζ (see Fig. 2). The narrow band containing limit cycle solutions that ranges between β_* and β_{**} moves upward and widens as parameter m is increased.

5. DISCUSSION

In order to compare our results with observational data, we estimate the free parameters of this model (β, ζ) for different groups of pulsating stars. For a fundamental mode in RR Lyrae or Cepheid stars, typical values are $\beta = 1$, $\zeta = 1$ as it is stated in SG88. However, for highly luminous pulsating stars the value of β decreases abruptly. We estimated for a typical β Cephei a value of $\beta \approx 0.17$ and $\zeta = 1$, for the most luminous classical Cepheids we found $\beta \approx 0.3$ and $\zeta = 6$, while for the least luminous classical Cepheids we obtained $\beta \approx 0.99$ and $\zeta = 0.24$ (Allen 1973, p. 216). This estimation was performed considering that if

$$Z = \frac{\mathscr{L}}{R_*^2 \rho T}, \tag{5.1}$$

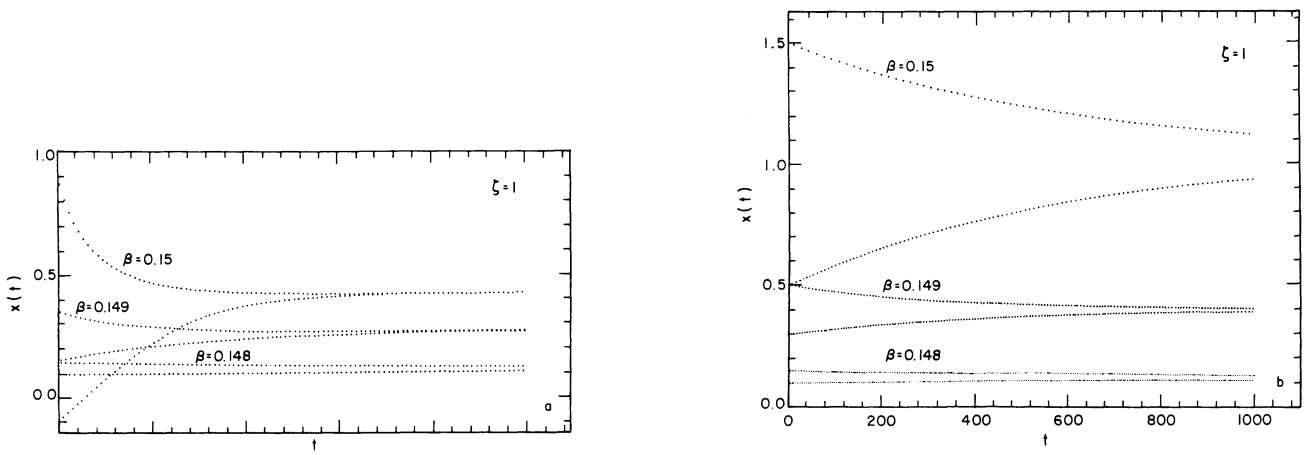

FIG. 5.—Relaxation toward the attractor $[x_{max}(t), t]$ for (*a*) the perturbative analysis and (*b*) the numerical integration

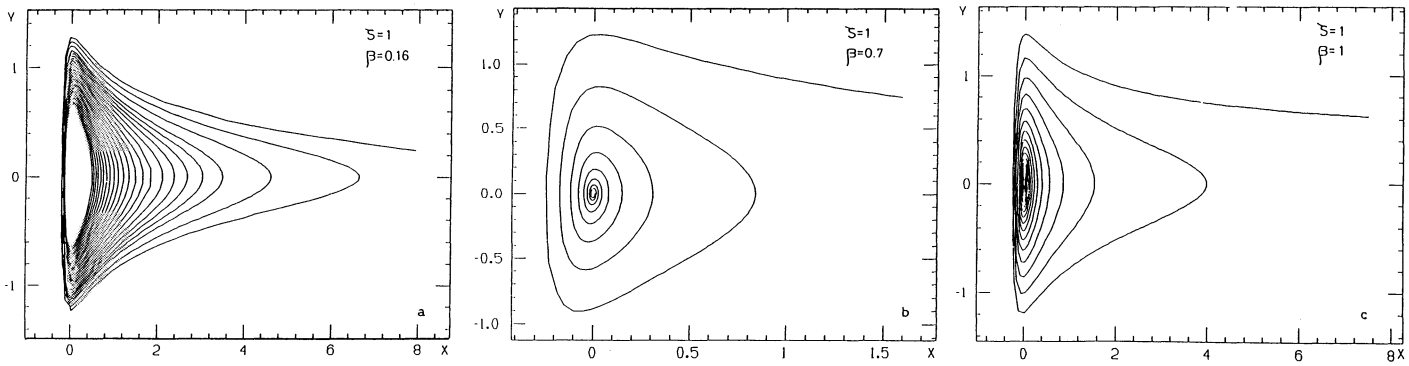

FIG. 6.—Ejection of the shell derived from the numerical integration in the y-x plane and for $\zeta = 1$ with (*a*) $\beta = 0.16$, (*b*) $\beta = 0.7$, and (*c*) $\beta = 1$

($\mathscr{L}$: luminosity, R_*: stellar radius, ρ: mass density, T: temperature), then

$$\beta = \frac{1}{(1 + K_1 Z)}, \qquad \zeta = K_2 Zm\left(\frac{R_*}{M}\right)^{1/2}, \tag{5.2}$$

where m is defined in SG88

$$K_1 = \frac{2m_H}{(9\pi c k_B)}, \qquad K_2 = \frac{m_H}{(6\pi k_B G^{1/2})}, \tag{5.3}$$

where k_B is the Boltzmann constant, c is the speed of light, and m_H is the hydrogen atom mass.

The amplitude of the attractors increases not only with β (Figs. 2 and 4*a*) but also as the value of ζ is raised (Figs. 2, 4*d*, and 7). To confirm this, we can schematically locate in Figure 2 the β Cephei stars as well as luminous and faint classical Cepheids. The pulsating velocity amplitudes for classical Cepheids are much larger than those for β Cephei, even when faint Cepheids have about the same ζ than β Cephei stars (but larger β) and the luminous Cepheids have almost the same β (but larger ζ). This is consistent with the empirical law for velocity amplitudes given in Allen (1973).

The nonadiabaticity of the pulsations causes a loss of energy per period which can be estimated through elementary arguments (Cox 1980). The e-folding time of this energy loss can be related to the relaxation time toward the limit cycle attractor. These damping times are summarized in Table 9.1 of Cox (1980) and are in qualitative agreement with our relaxation results in Figure 5*b*. We note that the relaxation time increases as β approaches either β_* or β_{**}. In the first case the cause is the proximity to the critical curve, while in the second it is because the trajectory enlarges near the ejection limit. For a star that is in the middle of the instability strip (say a W Virginis variable) Cox (1980) reports a relaxation time of around 10 periods, while either higher and lower β stars (luminous classical Cepheids and δ Scuti, respectively) have larger relaxation times, however, due to different (above mentioned) reasons. We remind the reader that, because of the simple physical model we adopted, these comparisons have to be considered at a speculative level.

As we mentioned, a chaotic evolution can be expected for irregular pulsating stars. Buchler & Kovacs (1987), employing a multishell model, found a strange attractor embeddable in a three-dimensional space. This suggests that a low-dimensional model can theoretically provide a good description or irregular variables. However, in the present model we did not find evidence of chaotic behavior. This is in accordance with the fast relaxation toward a two-dimensional manifold in the phase space (see Figs. 1 and 3*a*) and with the fact that chaos is not allowed to develop in two-dimensional manifolds (Eckmann & Ruelle 1985). The lack of irregularity in our model is a consequence of neglecting many degrees of freedom. For example, if the interaction of x, y, and h with the neglected degrees of freedom is simulated by adding noise terms to equations (2.1a)–(2.1c), the evolution becomes unpredictable. The noise effects will be more or less important according to whether the relaxation time toward the two-dimensional manifold is large or short compared to the pulsation period. Close to the bifurcation curve, even a low noise level may have an important consequence and give rise to the irregular features described by the models with more degrees of freedom.

6. CONCLUSIONS

The aim of this paper has been to look for limit cycle attracting solutions in models of pulsating stars. To this end we employed the equations derived in SG88, where radiation pressure effects are considered. We extend a standard nonlinear perturbative analysis (Iooss & Joseph 1980; Gomez et al. 1990) to obtain not only the features of the attractor but also information about the relaxation. We recovered the linear results of SG88 and obtained quantitative results concerning nonlinear features like shape and size of the attractor, corrections to the frequency, relaxation time, all of them as functions of two free parameters (β, ζ) which contain information about the star and the pulsating shell. The principal advantages of this technique compared to numerical integrations are (1) the attractor, that is, the solution for times going to infinity, is obtained directly without the necessity of carrying out long time integrations with high accuracy, and (2) a global view of the relevant characteristics of the limit cycle is obtained. The analytical results have been tested against numerical integration of the equations and found to be in satisfactory agreement, at least for β close to β_*. We have also found some interesting correspondences with observational data.

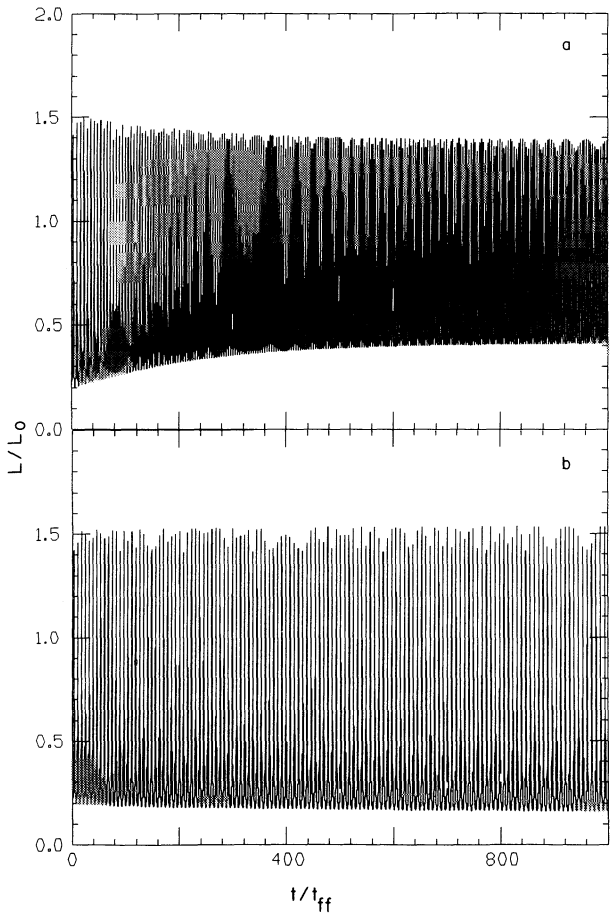

FIG. 7.—Dependence of the luminosity with time. The attractor luminosity is obtained for times longer that the relaxation one (final luminosity); (*a*) $\zeta = 1$, (*b*) $\zeta = 5$.

We can summarize our results as follows:

1. Sufficiently close to the bifurcation curve we have a very good agreement between the perturbative and the numerical results.
2. We have found a curve $\beta_{**}(\zeta)$ which corresponds to the physical situation of ejection of the shell. Thus the pulsating region lies between this curve and the critical one [$\beta_*(\zeta)$; see Fig. 2]. In the region above $\beta_{**}(\zeta)$, no limit cycle attractors are present. This behavior does not appear in SG88 due to the short integration times employed. However, the region containing limit cycle solutions, which ranges from β_* to β_{**}, depends on the parameter m and becomes wider for larger values of this parameter.
3. We compared our results with estimates coming from observational data and found some qualitative correspondence. The derived dependence of the velocity amplitude upon the free parameters [$\epsilon(\beta, \zeta)$] can explain the ordering of the observed amplitudes of highly luminous pulsating stars.

At a more speculative level, we remark the importance of noise effects close to the bifurcation curve as an alternative way of explaining the irregularity of some pulsating stars.

We would like to sincerely acknowledge an anonymous referee for many useful comments and suggestions that substantially contributed to improve the original version.

This work was supported by the Consejo Nacional de Investigaciones Cientificas y Tecnicas (CONICET, Argentina) under grant 9069/03.

REFERENCES

Allen, C. W. 1973, Astrophysical Quantities (London: Athlone)
Baker, N. H. 1966, in Stellar Evolution, ed. R. F. Stein & A. G. W. Cameron (New York: Plenum), 333
Buchler, J. R., & Goupil, M. J. 1984, ApJ, 279, 394
Buchler, J. R., & Kovács, G. 1987, ApJ, 320, L57
Cox, J. P. 1980, Theory of Stellar Pulsation (Princeton: Princeton Univ. Press)
Cox, J. P., & Stellingwerf, R. F. 1979, PASP, 91, 319
Eckmann, J. P., & Ruelle, D. 1985, Rev. Mod. Phys., 57(3), 617
Gomez, D., Sicardi Schifino, A., & Ferro Fontán, C. 1990, ApJ, 352, 326
Haken, H. 1983, Advanced Synergetics (Berlin: Springer)
Hassard, B. D., Kazarinoff, N. D., & Wan, W. H. 1981, Theory and Applications of Hopf Bifurcation (Cambridge: Cambridge Univ. Press)
Iooss, G., & Joseph, D. D. 1980, Elementary Stability and Bifurcation Theory (Berlin: Springer)
Stellingwerf, R. F. 1972, A&A, 21, 91
———. 1975, ApJ, 195, 441
Stellingwerf, R. F., & Gautschy, A. 1988, ApJ, 327, 801 (SG88)